



## Investigation of Inhibition Effect of Acrylic acid on C-Steel Corrosion in Sulfuric Acid Solutions

S. Abd El Wanees<sup>1,2\*</sup>, Salah Salem<sup>1</sup>, A.M.A Shehata<sup>3</sup> and M. Abd El Azim<sup>4</sup>

<sup>1,\*</sup>Chemistry Department, Faculty of Science, Tabuk University, Tabuk, Kingdom of Saudi Arabia  
Corresponding author, E-mail: s\_wanees@yahoo.com

<sup>2</sup>Chemistry Department, Faculty of Science, Zagazig University, Zagazig 44519, Egypt

<sup>3</sup>Chemistry Department, Faculty of Education 45111, Suez Canal University, Al-Arish, Egypt

<sup>4</sup>Department of Chemistry, Faculty of Science, Menoufia University, Menoufia, Egypt

### Abstract

Acrylic acid was tested as a corrosion inhibitor for C-steel in 0.5 M H<sub>2</sub>SO<sub>4</sub> using gasometry, weight loss, and galvanostatic polarization techniques. Polymeric film is built up by cyclic voltammetry technique. The potentiodynamic polarization is used to examine the inhibition effect with the coated polymeric film. The data obtained from the different techniques coincide in that acrylic acid is a good mixed-type inhibitor. The inhibition process is based on the adsorption of acrylic acid on the surface of C-steel according to Temkin's adsorption isotherm. The inhibition efficiency increases with inhibitor concentration and decreases with temperature. The thermodynamic parameters  $\Delta E$ ,  $\Delta H^*$ ,  $\Delta S^*$ , and  $\Delta G_{ads}^*$  were calculated to elaborate the mechanism of corrosion inhibition.

**Keywords**- Acrylic acid, Polymeric film, Corrosion inhibitor, Gasometry, Weight loss, Galvanostatic polarization and potentiodynamic .



## Council for Innovative Research

Peer Review Research Publishing System

**Journal:** Journal of Advances in Chemistry

Vol. 6, No. 3

editor@cirworld.com

[www.cirworld.com](http://www.cirworld.com), [member.cirworld.com](http://member.cirworld.com)



## I. INTRODUCTION

Corrosion process plays an important role in the fields of economics and safety. Various types of steel included in different industries (chemical and electrochemical industries, medical, nuclear, petroleum, power, and food production), and also in daily life. However, it suffers from a certain type of corrosion within some environments. For this reason, the electrochemical properties of carbon steel are the subject of many studies. The problems arising from acid corrosion require the development of various corrosion control techniques among which the application of chemical inhibitors has been acknowledged as most economical method for preventing acid corrosion [1–8]. A number of corrosion inhibitors of steel in aqueous solutions of mineral acids include unsaturated organic compounds, containing multiple bonds C=C that can easily attach hydrogen. The most studied groups of such compounds are acetylenic alcohols, many of which effectively retard corrosion of steel in hydrochloric acid solutions [9, 10].

Generally, it has been assumed that the first stage in the action mechanism of the inhibitors in an aggressive acid media is the adsorption of the inhibitors onto the metal surface. The processes of adsorption of inhibitors are influenced by the nature and surface charge of the metal, the chemical structure of organic inhibitors, the distribution of charge in the molecule, the type of aggressive media is the adsorption of the inhibitors onto the metal surface. The processes of adsorption of inhibitors are influenced by the nature and surface charge of the metal, the chemical structure of organic inhibitors, the distribution of charge in the molecule, the type of aggressive electrolyte, and type of interaction between organic molecules and the metallic surface [11-14]. Physical (electrostatic) adsorption and chemisorption's are the principle type of interaction between organic inhibitor and the metal surface [11-15].

Relatively, little work has been done on the inhibition effect of  $\alpha$ ,  $\beta$ -unsaturated carbonyl compounds for corrosion of different metals in acid solutions [15-20]. The aim of the present work is to investigate the inhibition effect of acrylic acid as an inhibitor on the corrosion of C-steel in 0.5 M  $H_2SO_4$  solution. The effect of concentration and temperature are studied through different experimental techniques, such as, gasometry, gravimetry and galvanostatic polarization. Also electro-polymerization of acrylic acid is used to build up a coated film on C-steel electrode by cyclic voltammetry method. The formed film is tested as a coat against corrosion of C-steel in 0.01 M  $H_2SO_4$  by potentiodynamic method.

## II. EXPERIMENTAL PROCEDURES

The steel electrodes were made from steel samples produced by Egyptian Steel Mill Co. (Helwan, Cairo), and have the following chemical composition in accordance with the Egyptian ASTM A615 Standard [21]:

C	Si	Mn	P	S	Fe
0.32	0.24	0.89	0.024	0.019	98.507 mass %

The steel specimens used for gasometry and gravimetry measurements were cut from steel sheets as regular cuboids with dimensions 5cm x 2cm x 0.3cm. For polarization measurements the working electrode was cut from cylindrical steel rod, welded with Cu-wire for electrical connection and mounted into glass tube of appropriate diameter using Araldite to offer an active flat disc shaped surface of 0.32 cm<sup>2</sup> geometric area. Prior to measurements, the surface of the steel was polished with SiC grinding papers, from 400 to 1200 grades, using a grinding machine (model Jean Wirtz TG 200, Germany). The electrodes were then degreased with acetone and finally washed with bi-distilled water before immersion in the test solution. Measurements were carried out at a constant temperature, 25± 1°C, except those related to the effect of temperature. The cell temperature was controlled using an ultra-thermostat type Polyscience (USA).

### A. Hydrogen evolution measurements

The test solution, 100 ml, was placed in flask of Mylius type [22 - 25] and the C-steel sample was introduced into the solution. The time was recorded and H<sub>2</sub> gas evolved was collected in the calibrated tube by the downward displacement of water over time interval of 60 min. A plot of volume of H<sub>2</sub> gas evolved per unit area against reaction time produced straight lines. The corrosion rate ( $r$ ) was assessed from the slope of these straight lines [22 - 25].

The surface coverage ( $\theta$ ) and the inhibition efficiency ( $IE\%$ ) of the inhibitor in 0.5 M  $H_2SO_4$  solution were calculated using equations [33]:

$$\theta = [1 - (r/r^0)] \quad (1)$$

$$\eta = \theta \times 100(2)$$

where  $r$  and  $r^0$  are the corrosion rates in the presence and absence of the acrylic acid, respectively.

### B. Weight loss measurements

Weight loss measurements were carried out as described elsewhere [22-24]. The cleaned degreased C-steel sheet was weighed before and after immersion in 100 ml of the test solution for the desired period of time. The average weight loss for each two identical experiments was taken and expressed in mg/cm<sup>2</sup>. The weight loss ( $\Delta W$ ) was calculated from the difference between the sample weights before ( $W$ ) and after ( $W'$ ) immersion in the test solution and the rate of corrosion,  $r$ , is expressed in mg cm<sup>-2</sup> min<sup>-1</sup> [23]. The inhibition efficiency was calculated from relation [15]:



$$\eta = [(r^{\circ} - r)/r^{\circ}] 100 \quad (3)$$

where  $r^{\circ}$  and  $r$  signify the corrosion rates in the absence and presence of inhibitor, respectively.

### C. Galvanostatic polarization measurements

The cell used for anodic and cathodic polarization measurements was previously described [24]. A conventional three-electrode system was used. A platinum sheet was used as an auxiliary electrode and the reference electrode was a saturated calomel electrode (SCE) with a Luggin capillary positioned close to the working electrode surface in order to minimize ohmic potential drop.

Prior to the galvanostatic polarization measurements, the steel electrode was immersed in the electrolyte under test until reaching a quasi-steady state corrosion potential which depends on the solution composition. Polarization process was started from low current values into the cathodic or the anodic directions. The current was changed manually and the potential was recorded using a digital multimeter. For each current value, the steady-state potential of the electrode was considered when its value did not change by more than 1 mV.

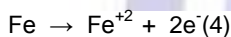
### D. Cyclic voltammetry and potentiodynamic anodic polarization measurements.

The cyclic voltammetry is used to form a polymeric film of acrylic acid on C-steel electrode in  $1 \times 10^{-2}$  M  $H_2SO_4$ , at a scan rate of 50 mV/s. The film become stable after 20 cycles, in presence of different concentrations of acrylic acid, between  $E_i = -1000$  mV and  $E_f = 0$  mV. The formed film on C-steel electrode is tested as an inhibitor against corrosion in  $1 \times 10^{-2}$  M  $H_2SO_4$  by potentiodynamic method.

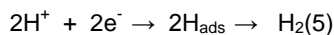
## III. RESULTS AND DISCUSSION

### A. Hydrogen evolution measurements

The technique of hydrogen gas evolution is used to follow the corrosion behaviour of C-steel in different concentration of  $H_2SO_4$  solutions. The data indicated that the hydrogen gas evolution starts after the elapses of a certain time from the immersion of C-steel in the test solution, which is depend on the acid concentration. This time is identified as the incubation period, which is the time needed by the acid to destruct the pre-immersion oxide film and start dissolution of the bare metal [25-27]. After the incubation period, the volume of the  $H_2$  gas evolved increases linearly with time due to the possible destruction of the porous film and the continuous dissolution of the bare metal, according to the reaction:



The accompanied cathodic reaction required to consume the electrons generated in the anodic reaction is shown in equation (4). In the acidic medium,  $H_{ads}$ , the atomic hydrogen adsorbed on the metal surface reacts by combining with other adsorbed H atoms to form  $H_2$  gas, which bubbles from the surface according to:



In Fig 1 the rate of dissolution of C-steel,  $r$ , under the prevailing experimental conditions, increases with increasing  $H_2SO_4$  concentration, according to the relation:

$$\log r = a + b \log C_{H^{+}} \quad (6)$$

where  $a$  and  $b$  are constants. The value of  $a = -1.23 \text{ ml cm}^{-2} \text{ min}^{-1}$  represents the log corrosion rate of C-steel at 1M  $H_2SO_4$  and  $b = 0.6 \text{ ml cm}^{-2} \text{ min}^{-1} \text{ decade}^{-1}$  represent the change in the rate of corrosion per unit concentration of  $H_2SO_4$ .

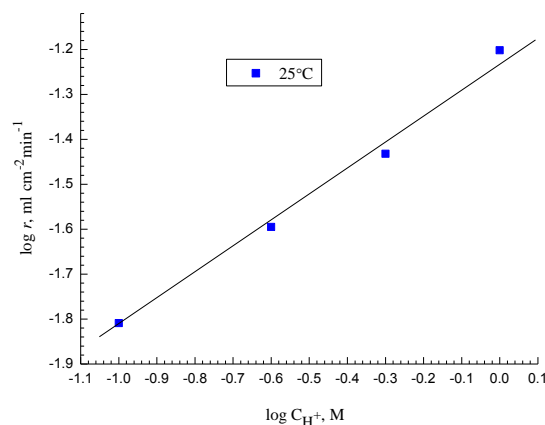


Fig. 1. Variation of the rate of corrosion of C- steel,  $r$ , with  $\log C_{H_2SO_4}$ .

The effect of additions of acrylic acid on the dissolution reaction of C-steel in 0.5 M H<sub>2</sub>SO<sub>4</sub> was indicated in Fig 2. The curves reveal that the incubation period is found to increase as the inhibitor concentration is increased, due to retardation of dissolution process. Fig 3 shows the plots of incubation period,  $\tau$ , as function of inhibitor concentration on a double logarithmic scale, which gives rise to a straight line relation satisfying the equation [28]:

$$\log \tau = A_1 + B_1 \log C_{inh} \quad (7)$$

where  $A_1$  and  $B_1$  are constants. The value of the constant  $A_1 = 2$  min represent the logarithm of the induction period when the inhibitor concentration equal 1M, while the value of the constant  $B_1 = 0.52 \log \text{ min/decade}$ .

The variation in the corrosion rate,  $r$ , of C-steel with the concentration of the inhibitor,  $C_{inh}$ , on a double logarithmic scale gives straight line, Fig 4, which satisfies the relation:  $r = a_1 - b_1 \log C_{inh}$  (8)

where  $a_1$  and  $b_1$  are constants. The value of  $a_1 = -0.047 \text{ ml cm}^{-2} \text{ min}^{-1}$  represents the logarithm of the rate of corrosion when inhibitor concentration equal 1M, while  $b_1 = -0.028 \text{ ml cm}^{-2} \text{ decade}^{-1}$ . The values of corrosion rates and inhibition efficiencies in the presence of different concentrations of the acrylic acid are shown in Table 1.

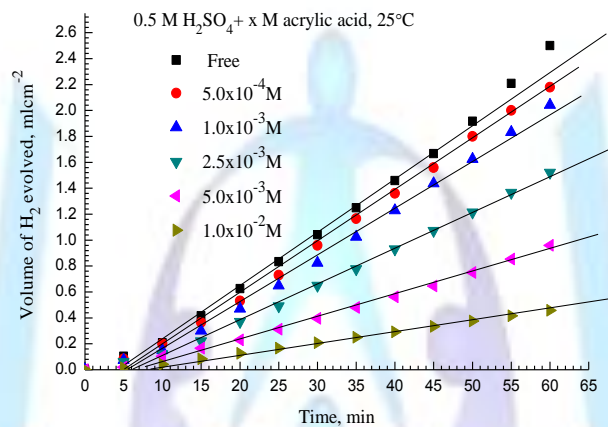


**Fig. 2.** Variation of the volume H<sub>2</sub> gas evolved with the immersion time for C-steel in 0.5M H<sub>2</sub>SO<sub>4</sub> in the absence and presence of different concentrations of acrylic acid, at 25°C.

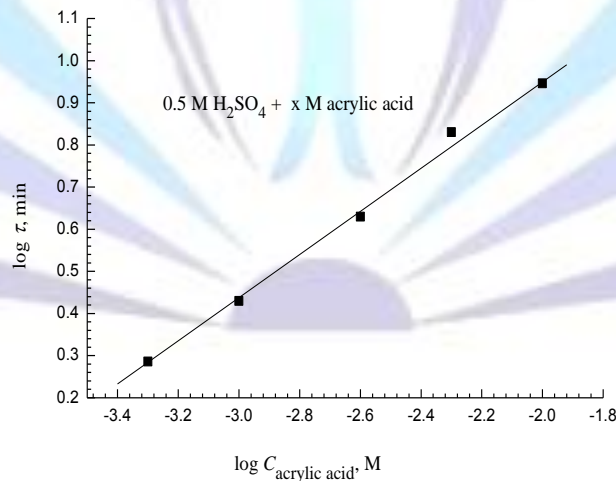


**Fig3.** Variation of the induction time,  $\tau$ , with  $\log C_{acrylic}$

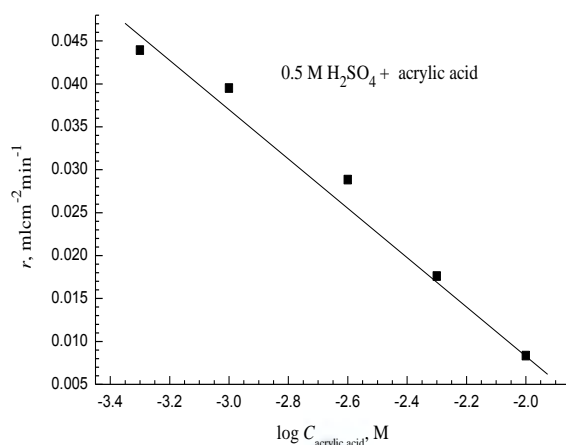


Fig 4.Variation of the rate of corrosion,  $r$ , of C- steel with  $\log C_{\text{acrylic}}$ .

### B. Weight loss method

Fig. 5 shows the variation of weight loss of C-steel with the immersion time in 0.5 M  $\text{H}_2\text{SO}_4$  in the absence and presence of different concentrations of acrylic acid, at 25 °C. This figure reveals that the inhibitor actually inhibited the induced corrosion of C-steel in  $\text{H}_2\text{SO}_4$  to an appreciable extent. It is clear that, the addition of acrylic acid increases the incubation period and decrease the rate of corrosion of C-steel by lowering the loss in the weight. It is easily to consider that the inhibition could be due to the adsorption of acrylic acid on the C-steel surface. The calculated inhibition efficiency values at different acrylic acid concentrations are given in Table 1.

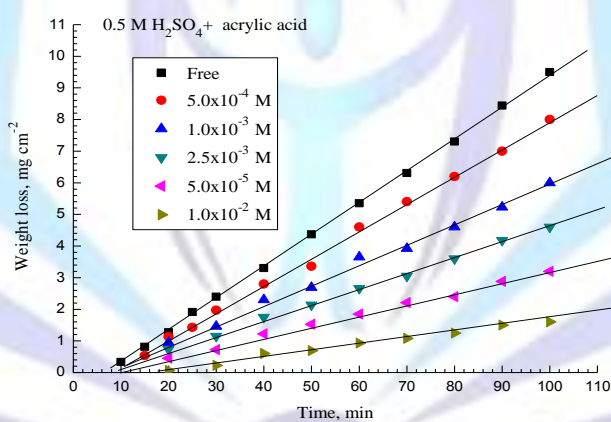


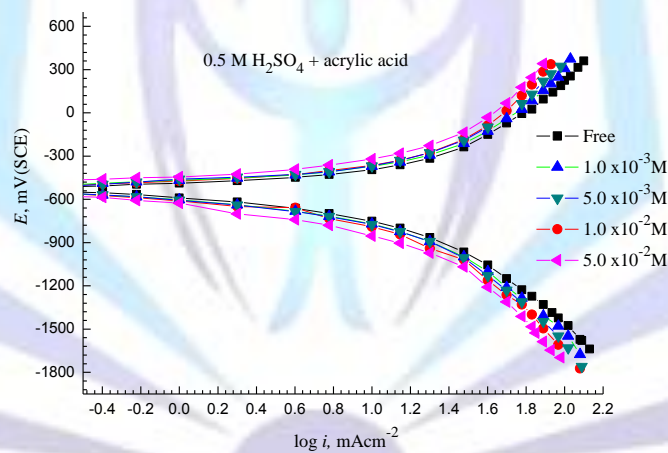
Fig 5.Variation of the weight loss with time for C- steel in 0.5 M  $\text{H}_2\text{SO}_4$  in the absence and presence of different concentrations of acrylic acid.

**Table 1. The rate of corrosion and inhibition efficiency values in presence of different concentrations of acrylic acid.**

Acrylic acid conc.	Gasometry method		Weight loss method,	
	$r$ , mlcm <sup>-2</sup> min <sup>-1</sup>	$\eta$	$r'$ , $\mu\text{gcm}^{-2}\text{min}^{-1}$	$\eta$
Free	0.042	---	101.00	---
5.0x10 <sup>-4</sup> M	0.038	9.5	86.3	14.5
1.0x10 <sup>-3</sup> M	0.034	18.7	65.2	35.4
2.5x10 <sup>-3</sup> M	0.025	40.2	48.6	51.9
5.0x10 <sup>-3</sup> M	0.016	61.9	34.1	66.2
1.0x10 <sup>-2</sup> M	0.007	82.6	19.4	80.8

### C. Galvanostatic polarization method

Galvanostatic polarization curves for the corrosion of C-steel in 0.5 M H<sub>2</sub>SO<sub>4</sub> in the absence and presence of different concentrations of acrylic acid is shown in Fig 6. It can be observed that both the cathodic and anodic reactions are suppressed in presence of acrylic acid, which suggests that the inhibitor exerted an efficient inhibitory effect on anodic dissolution of metal and cathodic hydrogen liberation reaction. The calculated values of corrosion current densities in presence of acrylic acid are found to decrease with inhibitor concentration, according to a double logarithmic relation, Fig 7.


**Fig 6. Galvanostatic polarization curves of C- steel in 0.5 M H<sub>2</sub>SO<sub>4</sub> in absence and presence of different concentrations of acrylic acid.**

Electrochemical parameters such as corrosion potential ( $E_{\text{corr}}$ ), corrosion current density ( $I_{\text{corr}}$ ), anodic and cathodic Tafel slopes ( $b_a$  and  $b_c$ ) obtained from the galvanostatic polarization measurements are listed in Table 2.

The inhibition efficiency,  $\eta$ , was calculated from following equation [29]:

$$\eta = [(I^0 - I) / I^0] 100 \quad (9)$$

where  $I^0$  and  $I$  signify the corrosion current densities in the absence and presence of the inhibitor, respectively. Inhibition efficiency,  $\eta$ , increases with the rise in the inhibitor concentration, Table 2. The inhibition efficiency,  $\eta$ , reaches a maximum value of 66.2 in presence of 0.01M acrylic acid while higher values,  $\geq 82.6\%$ , is obtained at the same inhibitor concentration, with using chemical measurements (weight loss and gasometry techniques), indicating the more reliability of chemical techniques.

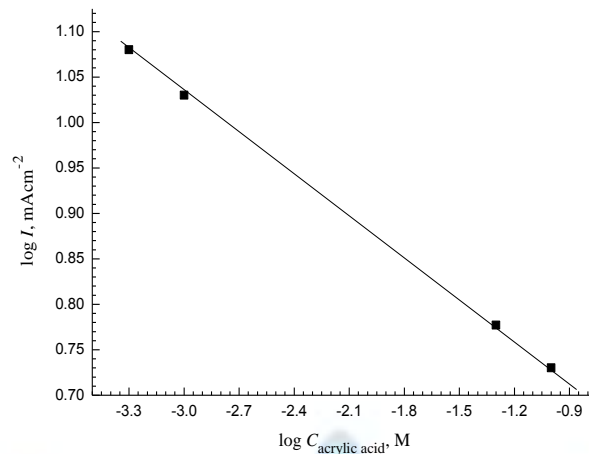


Fig7. Variation of the logarithm of the corrosion current density,  $I$ , of C- steel with  $\log C_{\text{acrylic}}$ .

Table 2. Electrochemical polarization parameters for the corrosion of steel in 0.5 M  $\text{H}_2\text{SO}_4$  containing various concentration of acrylic acid.

Inhibitor conc., M	$E_{\text{corr}}$ , mV, SCE	$b_a$ , mV dec <sup>-1</sup>	$b_c$ , mV dec <sup>-1</sup>	$I_{\text{corros}}$ , mA cm <sup>-2</sup>	$\eta$ (%)
Blank	-520	315	600	21.1	--
$1.0 \times 10^{-3}$	-516	314	598	12.0	21.1
$2.5 \times 10^{-3}$	-412	315	597	9.6	42.1
$5.0 \times 10^{-3}$	-413	312	597	7.0	57.7
$1.0 \times 10^{-2}$	-410	310	595	6.0	66.2

On the other point of view, it is seen from Table 2, that the value of the cathodic Tafel slope,  $b_c$ , does not change significantly with the increasing the inhibitor concentration, which indicates that the addition of acrylic acid does not change the mechanism of hydrogen evolution reaction [30]. Hydrogen evolution reaction has been reported to be generally the dominant local cathodic process in the corrosion of steel in aqueous acidic solutions, via  $\text{H}^+$  ion reduction [31]. The amounts of hydrogen gas evolved by the cathodic reaction are proportional to the corroded amounts of iron atoms. Also, it is seen from the data of Table 2 that the anodic slope,  $b_a$ , does not change significantly on increasing the concentration of acrylic acid, indicating its non-interference in the mechanism of anodic reaction. This indicates that the inhibitive action of acrylic acid may be considered due to its adsorption through the lone pair of electron density, of carbonyl group, and formation of barrier film on the electrode surface. The barrier film formed on the metal surface reduces the probability of both the anodic and cathodic reactions, which results a decrease in the corrosion rate [32].

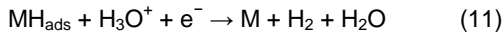
It can also be seen from Table 2 that there is no appreciable shift in the corrosion potential value ( $E_{\text{corr}}$ ) on the addition of acrylic acid to the corrosion medium. If the displacement in corrosion potential is more than  $\pm 85$  mV with respect to corrosion potential of the blank, then the inhibitor can be considered as a cathodic or anodic type [31]. However, the maximum displacement in the present study is  $\pm 10$  mV, which indicates that acrylic acid, is a mixed type inhibitor. As the concentration of the inhibitor increases, it is noticed that the corrosion potential shifts slightly toward more positive potential. This indicates that the inhibitor promotes passivation of steel through adsorption and decreases hydrogen gas evolution. The increase in the inhibition efficiency with the increase in inhibitor concentration is attributed to the increased surface coverage by the inhibitor molecules.

The liberation of hydrogen at the cathodic region can be formulated in three steps as follows [33]:

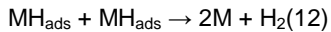
A primary discharge step (Volmer reaction)



An electrochemical desorption step (Heyrowsky reaction)



A recombination step (Tafel reaction)



The three steps formulated above do not take place as a single step, but combines with another. The presence of inhibitor may prevent the formation of  $MH_{ads}$  and suppress reaction [10] or prevent the electron transfer to  $H_3O^+$  and suppress reaction [11].

#### D. Potentiodynamic anodic polarization measurements.

The potentiodynamic anodic polarization curves of C-steel in 0.01 M sulfuric acid solution in the absence and presence of different concentrations of acrylic acid is shown in Fig 8. It is noteworthy to see that the anodic current densities are suppressed with the addition of acrylic acid, which suggests that the acrylic acid exerted an inhibitive effect towards the anodic dissolution of C-steel. The anodic current densities are found to decrease with increasing acrylic acid concentration.

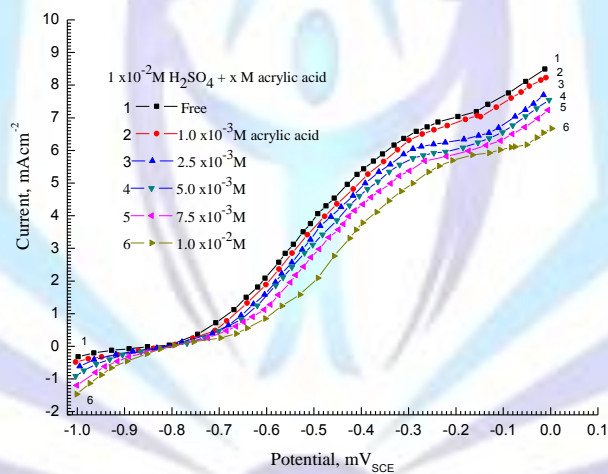


**Fig 8. Potentiodynamic anodic polarization curves of C- steel in 0.5 M  $H_2SO_4$  in the absence and presence of different concentrations of acrylic acid.**

Also, the potentiodynamic anodic polarization curves for C-steel electrode in presence of a coated film formed in 0.01 M sulfuric acid in presence of different concentration of acrylic acid is shown in Fig 9. The data of this figure clarified lowering in the anodic current densities values with increasing acrylic acid concentration. The values of the inhibition efficiency, calculated at a fixed potential, in case of a coated polymeric film is higher than that obtained from potentiodynamic data at a comparable concentration. This suggests that the electro-polymerized acrylic acid film on the surface of C-steel behaves as a good inhibitor.



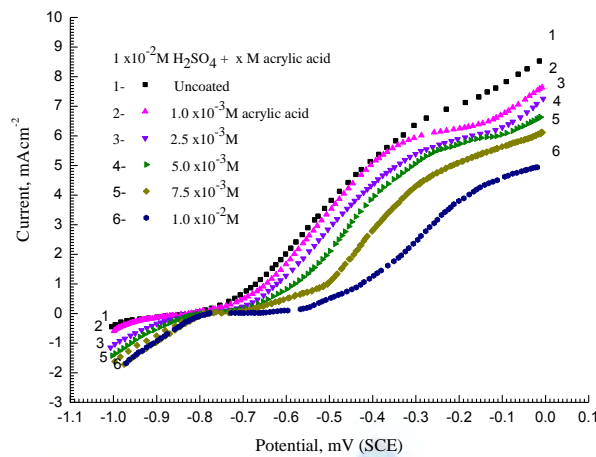


**Fig 9 Potentiodynamic anodic polarization curves of uncoated and coated C- steel in 0.01 M H<sub>2</sub>SO<sub>4</sub> in presence of polymeric coat of acrylic acid.**

### E. Effect of Temperature

The results of variation in the volume of hydrogen gas evolved with time for the corrosion of C-steel in 0.5 M H<sub>2</sub>SO<sub>4</sub> solutions in the absence and presence of different concentrations of acrylic acid at different temperatures is discussed. At all inhibitor concentrations, the inhibition efficiency of acrylic acid decreases with rising in temperature. The decrease in inhibition efficiency with temperature may be attributed to the higher dissolution rates of C-steel at elevated temperature and also a possible desorption of adsorbed inhibitor due to the increased solution agitation resulting from higher rates of hydrogen gas evolution. The higher rate of hydrogen gas evolution may also reduce the ability of the inhibitor to be adsorbed on the metal surface. The decrease in inhibition efficiency with the increase in temperature is also suggestive of physisorption of the inhibitor molecules on the metal surface [34].

The apparent activation energy ( $\Delta E_a$ ) for the corrosion process in the presence and absence of acrylic acid was calculated using Arrhenius law equation [35]:

$$\log r = B' - \Delta E_a / 2.303RT \quad (13)$$

where  $B'$  is Arrhenius pre-exponential constant which depends on the inhibitor concentration,  $R$  is the universal gas constant and  $T$  is the absolute temperature. The plot of  $\log r$  versus  $(1/T)$  gives a straight line with slope  $= -\Delta E_a / 2.303R$ , from which, the activation energy values for the corrosion process were calculated. The Arrhenius plots for the corrosion of C-steel in the presence of different concentrations of acrylic acid in 0.5 M sulfuric acid are shown in Fig 10.

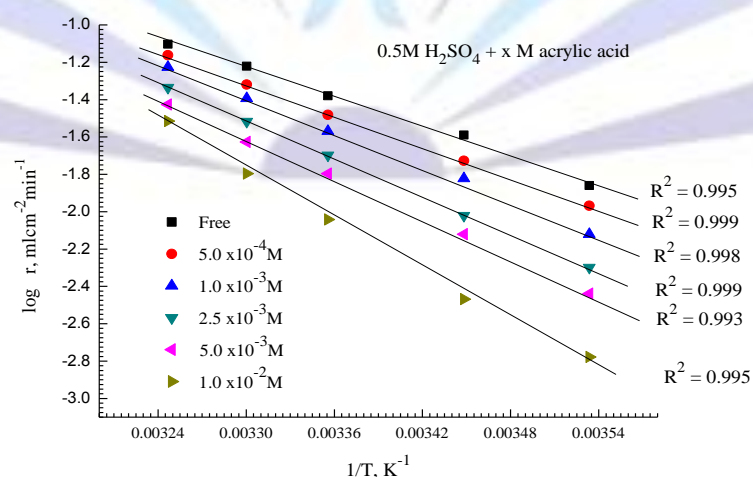


**Fig 10. Arrhenius plots for C-steel in 0.5 M H<sub>2</sub>SO<sub>4</sub> in absence and presence of different concentrations of acrylic acid.**

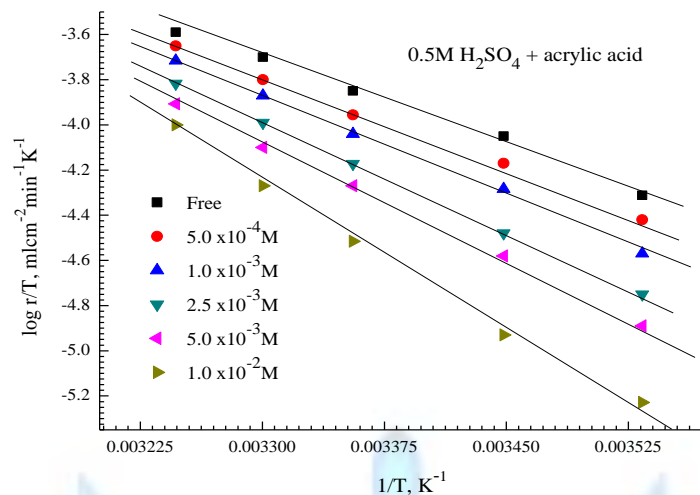


**Fig 11. Variation of  $\log(r/T)$  with  $1/T$  for C-steel in 0.5 M  $H_2SO_4$  in the absence and presence of different concentrations of acrylic acid.**

Table 3 shows the values of  $\Delta E_a$  for the corrosion of C-steel in 0.5 M  $H_2SO_4$  acid in the absence and presence of different concentrations of acrylic acid, the data obtained by the gasometry and weight loss techniques are consistent. In general,  $\Delta E_a$  values for the inhibited solutions (in the studied concentrations range) are higher than that of uninhibited one, and increase with increasing acrylic acid concentration. The increase in activation energy  $\Delta E_a$  indicates the retardation in corrosion rate which could have occurred because of adsorption of the inhibitors at the surface of the metal indicating a strong inhibitive action of acrylic acid in 0.5 M sulfuric acid by increasing the energy barrier for the corrosion process, emphasizing the electrostatic character of the inhibitor's adsorption on C-steel surface[30]. It is also indicated that the whole process is controlled by surface reaction, since the activation energies of the corrosion process are above  $20 \text{ kJ mol}^{-1}$ . The adsorption of the inhibitor on the electrode surface leads to the formation of a physical barrier between the metal surface and the corrosion medium, blocking the charge transfer, and thereby reducing the metal reactivity in the electrochemical reactions of corrosion.

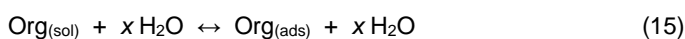
The entropy of activation ( $\Delta S^\ddagger$ ) and enthalpy of activation ( $\Delta H^\ddagger$ ) for the corrosion of C-steel were calculated from the transition state theory[34], using the formula:

$$r = (RT/Nh) \exp(\Delta S^\ddagger/R) \exp(-\Delta H^\ddagger/RT) \quad (14)$$

where  $h$  is Planck's constant, and  $N$  is Avagadro's number. The plots of  $\log(r/T)$  versus  $1/T$  in 0.5 M  $H_2SO_4$  in the presence of different concentrations of acrylic acid are shown in Fig 11. The calculated values of  $\Delta H^\ddagger$  and  $\Delta S^\ddagger$  are given in Table 4. The large negative values of entropy of activation ( $\Delta S^\ddagger$ ) implies that the activated complex is the rate determining step represents an association rather than dissociation, resulting in a decrease in randomness on going from the reactants to the activated complex [36]. The positive sign of the enthalpy reflects the endothermic nature of the steel dissolution process and suggesting the physical adsorption (physisorption). Generally, the negative sign of  $\Delta H^\ddagger$  indicates that the adsorption of inhibitor molecules is an exothermic process. An exothermic process signifies either physisorption or chemisorption or a combination of both. Typically, the standard enthalpy of physisorption process is less negative than  $41 \text{ kJ mol}^{-1}$ , while that of chemisorption process approaches to  $-100 \text{ kJ mol}^{-1}$ [37].

#### F. Adsorption Isotherm

The information on the interaction between the inhibitor molecules and the metal surface can be provided by adsorption isotherm. The adsorption of acrylic acid molecule on the metal surface can occur either through donor-acceptor interaction between the unshared electron pairs and/or  $\pi$ -electrons of inhibitor molecule and the vacant d-orbitals of the Fe atoms or through electrostatic interaction of the inhibitor molecules with already adsorbed sulfate ions. The adsorption bond strength is dependent on the composition of the corroded metal, inhibitor structure, concentration and orientation as well as temperature [6]. The adsorption of an organic adsorbate at metal/solution interface can be presented as a substitution adsorption process between the organic molecules in aqueous solution ( $Org_{aq}$ ), and the water molecules on metallic surface ( $H_2O_{ads}$ ), as given below [22]:





where  $x$ , the size ratio, is the number of water molecules displaced by one molecule of organic inhibitor,  $x$  is assumed to be independent of coverage or charge on the electrode.

The surface coverage ( $\theta$ ) was calculated from potentiodynamic polarization data using the equation <sup>[21]</sup>:

$$\theta = IE/100 \tag{16}$$

where  $IE(\%)$  is the percentage inhibition efficiency. The values of  $\theta$  at different concentrations of inhibitor in the solution ( $C_{inh}$ ) were applied to various isotherms including Langmuir, Temkin, Frumkin and Flory–Huggins isotherms. It was found that the data fitted best with the Temkin isotherm, i.e. [38]:

$$\exp(-2a\theta) = KC \tag{17}$$

where  $a$  is the lateral interaction term describing the molecular interactions in the adsorption layer and the heterogeneity of the metal surface, and  $K$  is the equilibrium constant of adsorption. Eq. 17 can be transformed into:

$$-2a\theta = \ln(KC) \tag{18}$$

$$-2a\theta = \ln K + \ln C \tag{19}$$

$$\theta = (1/-2a) \ln K + (1/-2a) \ln C \tag{20}$$

**Table 3.** The values of  $\Delta E_a$  for the corrosion of C-steel in 0.5 M  $H_2SO_4$  in the absence and presence of different concentrations of acrylic acid.

Acrylic acid conc.	$\Delta E_a$ , $kJ\ mol^{-1}$	
	Gasometry method	Weight loss method
Free	50.1	51
$5.0 \times 10^{-4} M$	53.4	54
$1.0 \times 10^{-3} M$	58.9	60
$2.5 \times 10^{-3} M$	64.5	66
$5.0 \times 10^{-3} M$	67.0	68
$1.0 \times 10^{-2} M$	84.4	88

**Table 4.** The values of  $\Delta H^\ddagger$  and  $\Delta S^\ddagger$  for the corrosion of C- steel in 0.5 M sulfuric acid in absence and presence of different concentrations of acrylic acid.

Inhibitor con.	$\Delta H^\ddagger$	$\Delta S^\ddagger$
(M)	( $kJ\ mol^{-1}$ )	( $J\ mol^{-1}\ K^{-1}$ )
Blank	49.2	-91.07
$5.0 \times 10^{-4}$	53.7	-57.98
$1.0 \times 10^{-3}$	57.1	-61.39
$2.5 \times 10^{-3}$	63.0	-42.97
$5.0 \times 10^{-3}$	64.0	-22.97
$1.0 \times 10^{-2}$	72.0	-17.99

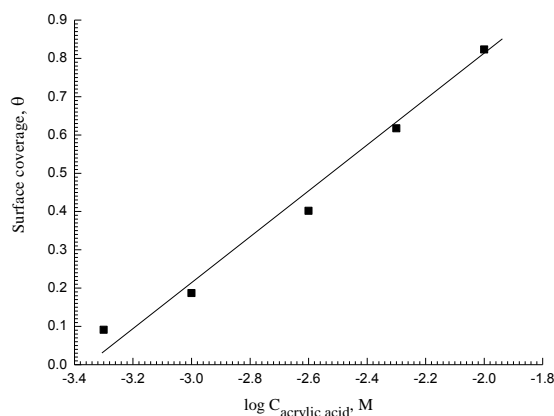


**Fig12. Temkin adsorption isotherm of acrylic acid on C- steel surface.**

Equations (18-20) are the different forms of Temkin isotherm. The regression between  $\theta$  and  $\ln C$  can give a straight line with a slope of  $1/(-2a)$  and an intercept of  $(1/-2a) \ln K$ , Fig 12. It is apparent that  $a$  can be calculated from the slope, with the calculated  $a$ , the value of  $K$  can be obtained from the intercept. The results obtained are shown in Table 5.

**Table 5. The values of  $K$  and  $a$  for adsorption of acrylic acid on C- steel in 0.5 M sulfuric.**

Temp.(°C)	$K (\times 10^4 M^{-1})$	$a$
17	3.990	-1.023
25	2.579	-0.860
30	2.825	-0.926
35	2.336	-0.850

It can be found that the linear regression coefficients are close to 1, meaning that the assumption is correct, i.e. the steel corrosion are inhibited by the adsorption of acrylic acid molecule, and the adsorption follows the Temkin adsorption isotherm. Furthermore, it can be concluded that the repulsion exists in the adsorption layer ( $a < 0$ ).

The standard free energy of adsorption, ( $\Delta G^\circ_{ads}$ ) was calculated using the relation [31]:

$$K = (1/55.5) \exp(-\Delta G^\circ_{ads} / RT) \quad (21)$$

where the value 55.5 is the concentration of water in solution in  $\text{mol l}^{-1}$ . The value of  $\Delta G^\circ_{ads}$  can be calculated. The standard free energy of adsorption ( $\Delta G^\circ_{ads}$ ) was found to be  $-35.2 \text{ kJ/mol}$ . The calculated value, less than the threshold value ( $-40 \text{ kJ/mol}$ ) required for chemical adsorption. This support the mechanism of physical adsorption, indicating that the inhibitor was adsorbed on the metal surface by physisorption process. The negative values indicate the spontaneity of the adsorption process and stability of the adsorbed layer on C-steel surface.

## V. CONCLUSION

- Acrylic acid acts as a good mixed inhibitor for the corrosion of C-steel in M  $\text{H}_2\text{SO}_4$  solution.
- Inhibition efficiency increases with increasing inhibitor concentration and decreases with raise in solution temperature.
- The values of apparent activation energy increases with the increase in the inhibitor concentration.
- Enthalpy of activation reflects the endothermic nature of C-steel dissolution process.
- Entropy of activation increases with increasing inhibitor concentration.
- The adsorption of acrylic acid on C-steel follows the Temkin adsorption isotherm.



## REFERENCES

- [1] Yaroslav, G., Avdeev; Yurii I. Kuznetsov, Aleksey K. Buryak (2013) *Corros. Sci.*, 69: 50-60.
- [2] Fragoza-Mar, L.; Olivares-Xometl, O.; Domínguez-Aguilar, M.A.; Flores, E.A.; Arellanes-Lozada, P.; Jiménez-Cruz, F. (2012) *Corros. Sci.*, 61: 71– 84.
- [3] Badr, G.E.(2009)*Corros. Sci.* 51: 2529–2536.
- [4] Okafor, P.C.;Zheng, Y.G. (2009) *Corros. Sci.* 51:850–859.
- [5]C. Kustu, K.C. Emregul, O. Atakol (2007) *Corros. Sci.* 49: 2800–2814.
- [6] Ostovari, A.;Hoseinie, S.M.; Peikari, M.;Shadizadeh, S.R.;Hashemi, S.J. (2009) *Corros. Sci.* 51: 1935–1949.
- [7] Bahrami, M.J.;Hosseinia, S.M.A. ;Pilvar, P.(2010)*Corros. Sci.* 52: 2793–2803.
- [8] Solomon, M.M. ;Umoren, S.A ; Udosoro, I.I. ; Udoh, A.P. (2010) *Corros. Sci.* 52: 1317–1325.
- [9] Podobaev, N.I.; Avdeev, Ya.G. (2004) *Protection of Metals* 40:7-13.
- [10] Bockris, J.O'M., Bo Yang (1991) *J. Electrochem. Soc.* 138: 2237–2252.
- [11] Granese, S.L. (1988) *Corrosion NACE* 44: 322–327.
- [12] Mimani, T.; Mayanna, S.M.; Munichandraiah, N. (1993)*J. Appl. Electrochem.* 33: 339–345.
- [13] Hukovic, M.A.; Grubac, Z.; Lisac, E.S. (1994) *Corrosion NACE* 50: 146–151.
- [14] Mahmoud, S.S.; El Mahdy, G.A. (1997) *Corrosion NACE* 53: 437–439.
- [15]Abd El Aal, E. E; Abd El Wanees, S. (2011) *Corrosion NACE* 67: 075003- 0750011.
- [16] Saliyan, V.R.; Adhikari, V. (2008) *Corros. Sci.* 50: 55–61.
- [17] Gao, J.; Weng, Y.; Salitanate, Feng, L.; Yue, H. (2009) *Petrol. Sci* 6: 201-207.
- [18] Quraishi, M.A.; Bhardwaj, V.; Rawat, J. (2002) *J. Am. Oil Chem. Soc.* 79: 603–609.
- [19] El Batouti, M. (1995) *Anti-Corros. Methods Mater.* 42: 15–18.
- [20] Quraishi, M.A.;Sardar, R.; Jamal, D. (2001) *Mater. Chem. Phys.* 71: 309–313.
- [21] Abd El Wanees, S.; Abd El Aal, E.E. (2010) *Corros. Sci.* 52: 338–344.
- [22] Yilmaz, A.B.; Dehri I.; Erbil, M. (2002) *Cem. Concr. Res* 32: 91–95.
- [23] Noor, E. A.; Al-Moubraki, A. H. (2008) *Mater. Chem. and Phys.* 110: 145-154.
- [24] Brett, C.M.A.; Gomes, I.A.R.; Martins, J.P.S. (1994) *Corros. Sci.* 36: 915–923.
- [25] El Shayeb, H.A.; Abd El Wahab, F.M.; El Meguid, E.A. (2001) *Br. Corros. J.* 36: 215–220.
- [26] Abd El Haleem, S.M.; Abd El Wanees, S.; Abd El Aal, E.E.; Farouk, A. (2012) *Corros. Sci.* 68: 1-13.
- [27] Abdallah, M. (2004) *Corros. Sci.*46:1981–1996.
- [28] Saleh, R. M.; Abd El Kader, J. M.; El Hosary A. A.; Shams El Din, A. M. (1975) *J. Electroanal. Chem. and Interf. Electrochem.* 62: 297-310.
- [29] Prabhu, R.A.; Shanbhag, A.V.; Venkatesha, T.V. (2007) *J. Appl. Electrochem.*37: 491- 497.
- [30] Avci, G. (2008) *Colloids Surf A* 317: 730-736.
- [31] Fekry, A.M.; Ameer, M. A. (2010) *Int. J. Hydrogen Energy* 34: 7641-7651.
- [32]W. Li, Q. He, S. Zhang, C. Pei, B. Hou, J. Appl. Electrochem. 38 (2008) 289-295.
- [33] Fekry, M.; Ameer, M.A. (2011) *Int. J. Hydrogen Energy.* 36: 11207-11215.
- [34] Geetha, M.P.; Nayak, J.; Shetty, A.N. (2011) *Mater. Chem. Phys.* 125: 628-640.
- [35] Poornima, T.; Nayak, J.; Shetty, A.N. (2011) *J. Appl. Electrochem.* 41: 223-233.
- [36] Fouda, A.S.; Heikal, F.E. ; Radwan, M.S. (2009) *J. Appl. Electrochem.* 39: 391-402.
- [37] Singh A.K; Quraishi M.A. (2010) *Corros. Sci.* 52:152-160.
- [38] Şahin, M.; Bilgiç, S. (1999) *Appl. Surf. Sci.* 147: 27-32.